Dielectric and Piezoelectric Properties of lead free ferroelectric $(Ba_{0.9}Ca_{0.1})$ $(Ti_{1-x}Sn_x)$ O3 (x=0.06, 0.08, 0.1) Ceramics

A Thesis Submitted in Partial Fulfillment of the

Requirements for the Degree of

Bachelor of Technology

in

Ceramic Engineering

By

SARBAJIT SANJAT KUMAR

(Roll No. 109CR0553)

Under the guidance of

Prof. R. Mazumder

Department of Ceramic Engineering,

National Institute of Technology,

Rourkela–769008, Odisha, India

CERTIFICATE

This is to certify that the thesis entitled, "**Dielectric and Piezoelectric Properties of lead free ferroelectric $(Ba_{0.9}Ca_{0.1})(Ti_{1-x}Sn_x)O_3$ (x=0.06,0.08,0.1) Ceramics**" submitted by **Sarbajit Sanjat Kumar** in partial fulfillment of the requirement for the award of Bachelor of Technology Degree in Ceramic Engineering at National Institute of Technology, Rourkela is an authentic work carried out by him under my supervision and guidance.

To the best of my knowledge, the matter embodied in the thesis has not been submitted to any other University/ Institute for the award of any Degree or Diploma.

Date:

Prof. Ranabrata Mazumder

Department of Ceramic Engineering
National Institute of Technology,
Rourkela – 769008
Odisha, India

ACKNOWLEDGEMENT

First and foremost, I would like to dedicate my project thesis to my beloved parents for their love and support throughout my life.

I offer my sincerest gratitude to my supervisor Dr R. Mazumder, Department of Ceramic Engineering, National Institute of Technology Rourkela for introducing the present topic and for his inspiring guidance, patience and valuable suggestions throughout this project work.

I am deeply grateful to Prof. S.K Pratihar, Head and Department of Ceramic Engineering for his encouragement and help to carry out the thesis work.

I must also acknowledge my gratitude to all the faculty members and staff members of Department of Ceramic Engineering, NIT Rourkela.

I am also thankful to Mr. Ganesh Kumar Sahoo, Ms. Prativa Adhikari and other research scholars in the Department of Ceramic Engineering for providing all joyful environment in the lab and helping me out in different ways.

I would like to mention my special thanks to Mr. Abhinaya Sreeram, M.Tech(R) scholar, Department of Ceramic Engineering for his encouragement, interest and freely given time throughout this project.

Date: SARBAJIT SANJAT KUMAR

ABSTRACT

In the present project, $(Ba_{0.9}Ca_{0.1})(Ti_{1-x}Sn_x)O_3$(x=0.06, 0.08 and 0.1) lead-free ceramics were synthesized by conventional solid state route. XRD analysis of calcined sample shows formation of perovskite phase. The BZT- BCT ceramic samples were calcined and sintered at lower temperatures 1300^oC and 1350^oC, respectively which was lower compared to the previous reported literature. The average particle size was found to be 0.5-1µm from FESEM analysis. Dielectric measurements of the sintered sample were carried out for the compositions over the frequency range of 42 Hz -1MHz and temperature range from 28^oC to 100^oC. Each sample showed a maximum dielectric constant at the Curie temperature (T_C). With increase in the value of 'x' from 0.06 to 0.1 the composition had shown decrease in the Curie temperature values which were 85^oC, 40^oC and 30^oC respectively. The dielectric and piezoelectric properties of our sintered samples are comparable to those of conventionally prepared $(Ba_{0.9}Ca_{0.1})(Ti_{1-x}Sn_x)O_3$ ceramics reported earlier. These ceramics are potential candidates for the lead-free piezoelectric applications.

List Of Figures

List Of Tables

Page No.

CONTENTS

CHAPTER-1

INTRODUCTION

1. Introduction

Piezoelectric ceramics are widely used as actuators, resonators, and spark igniters. Lead zirconate titanate (PZT) ceramics are the most widely used piezoelectric materials due to their superior piezoelectric properties close to the morphotropic phase boundary (MPB) between rhombohedral and tetragonal phases. Nevertheless, PZTs are not environmental friendly for their lead oxide toxicity. Because of global environmental concerns, there is currently a strong push to invent lead-free piezoelectrics for device engineering [1-3].

During the last two decades, a series of typical lead-free systems such as $BaTiO_3$ (BT), $(Bi_{0.5}Na_{0.5})TiO_3$ (BNT) and $(K_{0.5}Na_{0.5})NbO_3$ (KNN) based ceramics have been investigated to substitute the PZT[4-5].Till date the properties of developed lead free piezoelectrics are not comparable to that of PZT based compositions. KNN based system suffers from alkali evaporation during sintering, poor sinterability, moisture sensitivity of the raw materials. BNT based system suffers from high leakage current. Among those systems, the BaTiO3-based ceramics which exhibit excellent electric properties are one of promising candidate to replace the PZT-based ceramics.

Recently, invention of high dielectric and piezoelectric properties in $0.5Ba(Zr_{0.2}Ti_{0.8})O_3$–$0.5(Ba_{0.7}Ca_{0.3})TiO_3$(BZT–0.5BCT) [This composition can be represented by $(Ba_{0.85}Ca_{0.15})(Zr_{0.1}Ti_{0.9})O_3$], attracted much attention to develop BaTiO3- based leadfree piezoelectric materials. The enhanced dielectric and piezoelectric properties are due to the coexistence of different polymorphic phases. Sn-modifications in BaTiO3 produce similar effect like Zr-substitution [6]. It will be interesting to study whether similar high dielectric and piezoelectric properties can be obtained in Sn, Ca co-modified BaTiO3.

1.1 $BaTiO_3$ Ceramics

$BaTiO_3$ is isostructural with the mineral perovskite ($CaTiO_3$) and so is referred to as ‘perovskite’. In perovskite structure, ABO_3 where ‘A’ and ‘B’ are cation elements or mixture of two or more cation elements. In the ideal perovskite crystal structure shown in Fig 1.1, if ‘A’ atom is taken at the corner of the cube, then ‘B’ atom resides in the body centre and an oxygen atom at each face Centre of the cube.

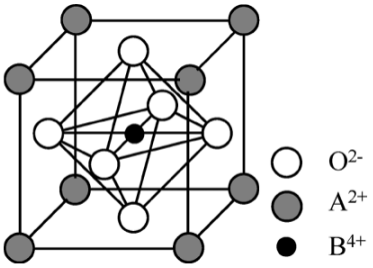

Figure 1.1 Schematic view of the perovskite ABO_3 unit cell for cubic $BaTiO_3$

For $BaTiO_3$, above its Curie point (approximately 130°C) the unit cell is cubic. Below the Curie point the structure is slightly distorted to the tetragonal form with a dipole moment along c direction. Other transformations occur at temperatures close to 0°C and -90°C: below 5°C the unit cell is orthorhombic with the polar axis parallel to a face diagonal and below -90°C it is rhombohedral with the polar axis along a body diagonal. The various phases of $BaTiO_3$ is shown in fig 1.2

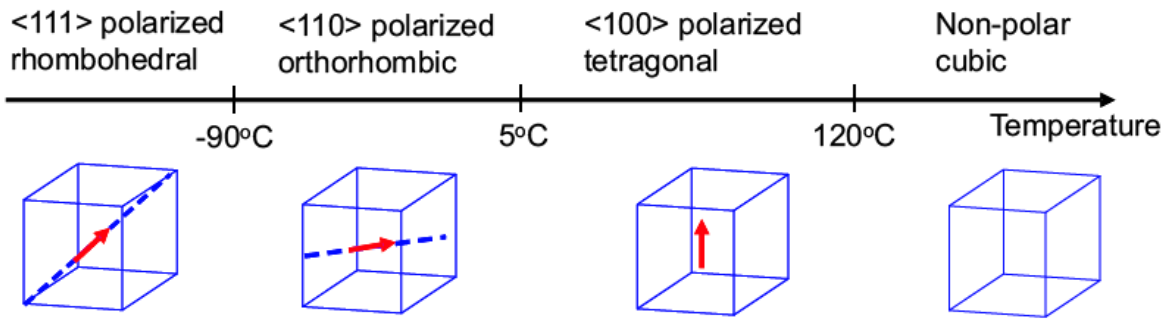

Figure 1.2 various phases of $BaTiO_3$.

Variation of dielectric constant, spontaneous polarization and lattice parameter in different phases of $BaTiO_3$ is shown in the fig.1.3. The tetragonal phase of $BaTiO_3$ has been the object of most investigations as this phase is stable at and above room temperature.

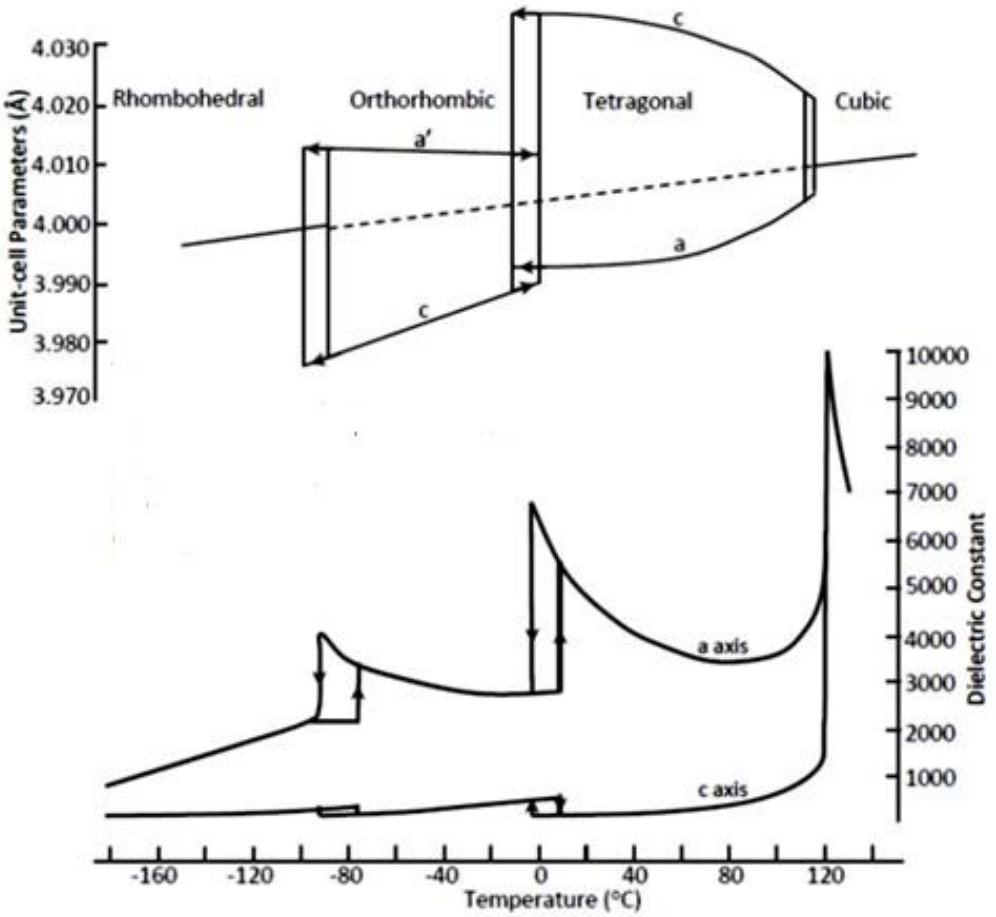

Figure 1.3 various lattice parameters and dielectric constant in different phases of $BaTiO_3$

A large number of A/B site substitutions in barium titanate based solid solutions have been investigated for optimizing the dielectric properties and shifting the Curie temperature in desired temperature range for applications. These includes Sr^{2+}, Ca^{2+},Bi^{3+} etc. at A site and Zr^{4+}, Sn^{4+}, Nb^{5+}etc. at B site [1]

1.2 Curie temperature (T_C)

Ferroelectric crystals exhibit electric dipole moments even in the absence of an external electric field below a certain temperature and a paraelectric behavior above this temperature. This temperature of structural phase transition from a high-temperature non ferroelectric

paraelectric phase to a low-temperature ferroelectric phase is called the Curie temperature (Tc). [7]

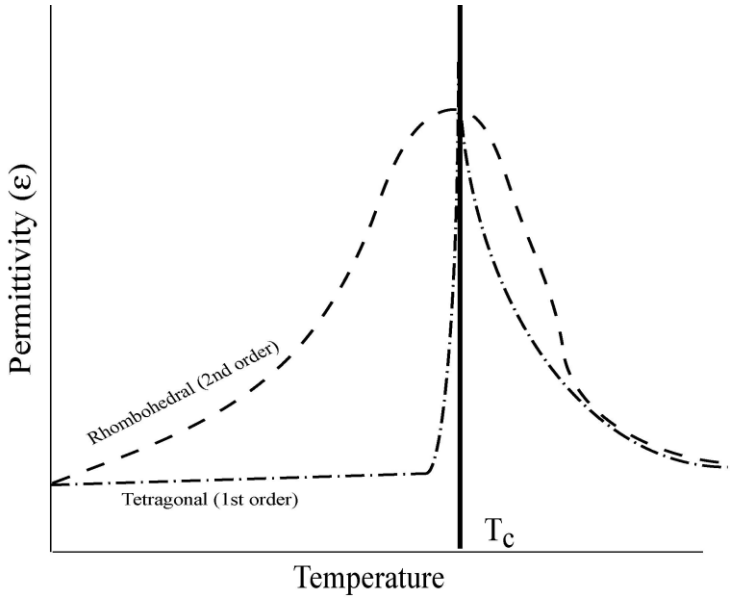

Figure 1.4 Idealized permittivity of ferroelectric material as a function of temperature.

In ferroelectrics dominated by a displacive phase transition, such as perovskite materials, the temperature dependence of the permittivity varies for 1st and 2nd order phase transitions. Fig. 1.4 illustrates the temperature dependence of the permittivity for displacive ferroelectric materials exhibiting first or second order phase transitions. Second order phase transitions, which are common for rhombohedral compositions, are generally characterized by a broad peak in permittivity. Ferroelectrics undergoing first order phase transitions, typical of tetragonal perovskite materials, however show a fairly flat permittivity with increasing temperature right up to the T_c.

The reciprocal permittivity 1/ε is known to be linear with respect to the temperature in a wide range in the paraelectric phase (so-called Curie-Weiss law),

$$\varepsilon = \frac{C}{T - T_0}$$

where C is the Curie-Weiss constant and T_0 the Curie-Weiss temperature. T_0 is slightly lower than the exact transition temperature Tc. For displacive transitions (e.g., $BaTiO_3$, $PbTiO_3$, $KNbO_3$), the Curie Constant is very high (~ 10^4 – 10^5K) and the paraelectric phase is

microscopically nonpolar. For order-disorder transition (e.g., TGS, KH_2PO_4), the Curie constant is of the order of T_0 and the paraelectric phase is nonpolar on macroscopic or thermally averaged sense. The reorientable component of the spontaneous polarization of ferroelectric materials falls to zero at the Curie temperature.

1.3 Hysteresis loop

Hysteresis loop is the most generally accepted method to understand ferroelectric materials [8]. In principle, every ferroelectric material has its own unique hysteresis loop, as a fingerprint. Through the hysteresis loops, the ferroelectricity could be identified directly. Fig.1.5 is a typical ferroelectric hysteresis loop, through which the characteristic parameters, such as spontaneous polarization (Ps), remnant polarization (Pr) and coercive field (Ec) can be determined. Owing to the requirement of the energy minima, the grains in polycrystalline materials are always splitting into many domains. The directions of the domains are randomly distributed in such a way to lead to zero net macroscopic polarization. When the external field exceeds the Ec, the polycrystalline ferroelectric ceramic may be brought into a polar state. Macroscopic polarization is induced gradually by increasing the electric field strength. The drastic variation in the polarization in the vicinity of Ec is mainly attributed to the polarization reversal (domain switching), while at high field end, the polarization is saturated and the material behaves as a linear dielectric. When the electric field strength starts to decrease, some domains would back-switch, but at zero field the net polarization is nonzero, leading to the remnant polarization Pr. To obtain a zero polarization, an electric field with opposite direction is needed. Such field strength is called the coercive field (or coercivity). With increasing the opposite field strength, a similar rearrangement of the polarization is observed in the negative field part. For ferroelectric materials, the spontaneous polarization Ps may be estimated by intercepting the polarization axis with the extrapolated linear segment.

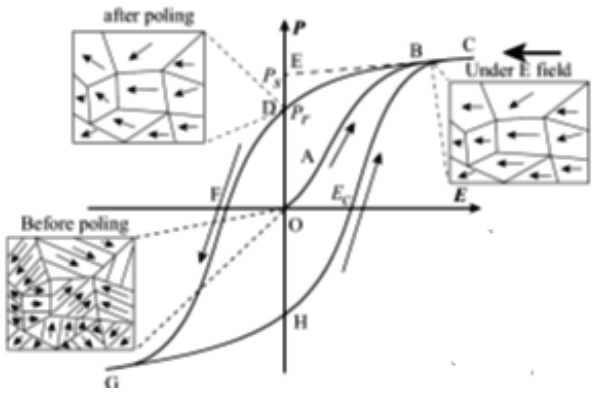

Figure 1.5 A typical hysteresis loop in ferroelectrics and corresponding domain reversal (polarization rotation)

1.4 Lead free ferroelectric ceramics

Till date the properties of developed lead free piezoelectrics are not comparable to that of PZT based compositions. $BaTiO_3$ is a model ferroelectric mostly utilized for capacitor and thermistor applications [2, 9, 10].The breakthrough made by Xue et al. in $BaTiO_3$-based ceramics with co-dopants of Ca and Sn has offered a significant impact on the development of lead-free piezoceramics[11**].** The pure $BaTiO_3$ ceramics are normally associated with a poor piezoelectric coefficient d_{33} as low as 191 pCN^{-1} [2], the value reported by Xue et al.[11] reached more than 500 pC/N, comparable to that of soft PZT ceramics. The proposed origin of high piezoelectricity was formation of MPB between $Ba(Ti_{0.88}Sn_{0.12})O_3$-$0.3(Ba_{0.7}Ca_{0.3})TiO_3$[BTS- 0.3BCT].

.

CHAPTER-2

LITERATURE REVIEW

2.1 Literature Review:

Calcium is most commonly doped in the $BaTiO_3$ ceramics. It has been reported that Ca^{2+} can occupy both Ba^{2+} and Ti^{4+} sites [12-14] Phase relations in $BaTiO_3$–$CaTiO_3$ system were studied by Devries and Roy [15]. According to their phase diagram, $CaTiO_3$ up to ~18mol% forms a homogenous solid solution with $BaTiO_3$ at 1400°C.

Berlincourt and Kulesar [16] et al. found that the Ca substitution in $BaTiO_3$ ceramic caused only negligible changes in the Curie temperature but strongly lower the tetragonal–orthorhombic transition temperature, which improved the temperature stability of piezoelectric/electostrictive properties.

Mitsui et al and Jaffe et al. [17,2], from the dielectric and X-ray diffraction (XRD) studies, demonstrated that the Curie point of $Ba_{1-x}Ca_xTiO_3$,(BCT) increases from 130°C for pure $BaTiO_3$ up to 136.1°C for x=0.08 and then decreases slightly for continuous increase in Ca concentration up to 25%.

Zhang et al reported the phase transition temperature of Ca^{2+} doped $BaTiO_3$ ceramics. Phase transition temperature of A and B site Ca^{+2} doped $BaTiO_3$ ceramics are shown in Fig 2.1 [18]. Low level of Ca^{2+} doping on B site (≤4at %) in $BaTiO_3$ have a dramatic and detrimental effect on Tc and grain conductivity. Ca^{2+} doping on A-site in $BaTiO_3$ showed the desired enhancement of Tc.

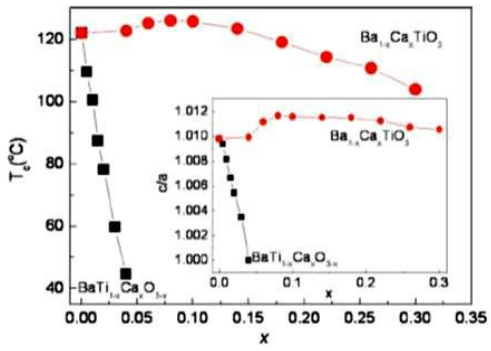

Figure 2.1 Phase transition temperature vs Ca content for $Ba_{1-x}Ca_xTiO_3$ (BCT), and $BaTi_{1-x}Ca_xO_{3-x}$(BTC) Inset shows c/a vs Ca content for BCT and BTC.

Sn^{4+} replaces Ti^{4+} and forms a $Ba(Ti_{1-x}Sn_x)O_3$, BSnT solid solution, which shows diffuse phase-transition behavior and a controllable curie temperature [19]. The Partial replacement of Ti^{4+} with Sn^{4+} decreases the Curie temperature (Tc). $BaSn_{0.3}Ti_{0.7}O_3$ was a typical relaxor ferroelectric and

$BaSn_{0.2}Ti_{0.8}O_3$ was a quasi-relaxation ferroelectric that is intermediate between a normal ferroelectric and a relaxor ferroelectric in its properties [20]. The paraelectric–ferroelectric phase transition temperature of $BaSn_{0.1}Ti_{0.9}O_3$ and $BaSn_{0.15}Ti_{0.85}O_3$ were 40°C and 5°C, respectively [21].

Li et al[22] studied Large Piezoelectric Coefficient in $(Ba_{1-x}Ca_x)(Ti_{0.96}Sn_{0.04})O_3$ Lead-Free Ceramics and found that At room temperature, a polymorphic phase transition from orthorhombic phase to tetragonal phase was identified in the composition range of $0.01 < x < 0.03$. They used solid state synthesis route for powder preparation and calcined the powder at 1200^0C for 4hrs & sintering temperature was used 1500^0C for 4 hr. Polarization versus electric field of the BCST ceramics can be seen that the coercive fields increase with increasing Ca content. The remnant polarizations increase to a maximum value of 13.2μC/cm^2 at x=0.02 and then decrease. At a curie temperature of around 80^0C a maximum value of relative permittivity of 15000 was observed.

W. Li et al. [23] studied Enhanced ferroelectric properties in $(Ba_{1-x}Ca_x)(Ti_{0.94}Sn_{0.06})O3$ lead-free ceramics and found that at room temperature a polymorphic phase transition (PPT) from orthorhombic phase to tetragonal phase was identified in the composition range of $0.02 < x < 0.04$.They used solid synthesis route for powder preparation and calcined the powder at 1200^0C for 4hrs & sintering temperature was used 1500^0C for 4 hr for 15mm dia pellets. SEM micrographs of the BCST ceramics at x= 0.01 showed that inhomogeneous and some pores exist in the grain boundary. For the samples at x= 0.02 and 0.03, the microstructure is homogeneous and no pore exists in the grain boundary. For the sample at x= 0.04, the microstructure is inhomogeneous and the grain size becomes small. With the increase of Ca content, remnant polarizations of the BCST ceramics increase to a maximum value 12.22lμC/cm^2 . At a curie temperature of around 80^0C a maximum value of relative permittivity of 6900 was noted for x= 0.02.

Zhu et al [24] studied Enhanced Piezoelectric Properties of $(Ba_{1-x}Ca_x)(Ti_{0.92}Sn_{0.08})O3$ Lead-Free Ceramics and found that At room temperature, a polymorphic phase transition from orthorhombic phase to tetragonal phase was confirmed by the XRD patterns in the composition range of $0.04 \leq x \leq 0.06$. They used solid synthesis route for powder preparation and calcined the powder at 1300^0C for 4hrs & sintering temperature was used 1480^0C for 4 hr . SEM micrographs

of the ceramics show that the small grains grow close to the big ones with increasing x from 0.00 to 0.05. TC of samples was increased from 58°C to 64°C by adding Ca^{2+} ions from 0.00 to 0.06. For the ceramic at x=0.05 at room temperature, whereby excellent electrical properties: €r =23000, P_r =10.65lμc/cm2.

2.2 Summary of literature review and scope of the work:

- Barium titanate ($BaTiO_3$)-based ceramics is considered to be one of promising lead-free ferroelectric ceramics of interest in the context of capacitor and piezoelectric transducer. However, the $BaTiO_3$ in its pure form has exhibits the small permittivity, the poor piezoelectric properties and low Curie temperature have been the main obstacle for their wider commercial application.
- Chemical substitutions at the Ba^{2+} and Ti^{4+} sites are made to tailor the properties to meet a variety of device and performance requirements.
  - Attempts to obtain good dielectric and piezoelectric property of BaTiO3-based ceramics by co-doping Sn and Ca ions have been studied. It is to be mentioned that optimization of the doping content is important to obtain good piezoelectric property in the (Ba,Ca)(Ti,Sn)O3 system.
  - It is reported that $(Ba_{0.9}Ca_{0.1})(Ti_{0.94}Sn_{0.08})O_3$ solid solution shows good dielectric and piezoelectric property. Keeping Ca-content fixed, variation of Sn content has to be studied.
  - Solid state synthesis route is very easy and cheapest route.

In the present work $(Ba_{0.9}Ca_{0.1})(Ti_{1-X}Sn_X)O3$ (x=0.06, 0.08, 0.1) lead-free ceramics were fabricated by conventional solid state synthesis method and their structure, densification, electrical properties were studied systematically.

2.3 Statement of the Problem:

1. To synthesize a phase pure solid solution of $(Ba_{0.9}Ca_{0.1})(Ti_{1-X}Sn_X)O_3$ by solid state reaction route taking x=0.06,0.08 & 0.1
2. To study the sintering behavior of $(Ba_{0.9}Ca_{0.1})(Ti_{1-X}Sn_X)O_3$ by varying sintering temperature.
3. To study the dielectric behavior of sintered ceramics.
4. To study the P-E loop of ceramics.
5. To study the piezoelectric properties of ceramics at room temperature.
6. To study the microstructure by FESEM.

CHAPTER-3

EXPERIMENTAL WORK

3. Experimental Procedure

3.1 The raw materials used for synthesis of $(Ba_{0.9}Ca_{0.1})(Ti_{1-X}Sn_X)O_3$:

- Barium Carbonate($BaCO_3$)
- Calcium Carbonate($CaCO_3$)
- Titanium Dioxide(TiO_2)
- Stannic Oxide(SnO_2)

3.2 Powder preparation by solid state synthesis:

Solid state synthesis method was adopted to produce powder for samples. **$(Ba_{0.9}Ca_{0.1})(Ti_{1-X}Sn_X)O_3$** was prepared with x=0, 0.06, 0.08, 0.1. For powder preparation high purity Sigma Aldrich chemicals of barium carbonate ($BaCO_3$) powder, calcium carbonate ($CaCO_3$) powder, titanium dioxide (TiO_2) powder, and stannic oxide (SnO_2) powders were used. The powders were weighed and milled for 12h, using pot milling with zirconia balls and isopropyl alcohol media after which the mixture was dried under IR lamp. For a batch of 15gm 60ml of propanol was added.

Different sample compositions:

1. For 15 gms $(Ba_{0.9}Ca_{0.1})(Ti_{1-X}Sn_X)O_3$ sample compositions –

Table 1

	X=0.06	**X=0.08**	**X=0.1**
$BaCO_3$	11.6990 gm	11.6275 gm	11.5560 gm
$CaCO_3$	0.6592 gm	0.6552 gm	0.6512 gm
TiO_2	4.9451 gm	4.8103 gm	4.6768 gm
SnO_2	0.5955 gm	0.7893 gm	0.9805 gm

3.3 Calcination of powder:

The powder was ground in agate mortar and dried properly and then calcined in alumina crucible at 1300^0C for 4 hours. The calcinations help in driving out all volatile and gaseous material from powder. After calcination the powders were ground and stored.

3.4 Particle Size Analysis

A laser diffraction method with a multiple scattering technique has been used to determine the particle size distribution of the powder. The relation between particle size and scattering angle is such that large particles scatter light at low angles while small particles scatter light at high angles. In order to find out the particles size distribution, the $BaTiO_3$ based powders were dispersed in water by ultrasonic processor [Vibronics, model:VPLP1].Then experiment was carried out in computer controlled particle size analyzer [ZETA Sizers Nanoseries (Malvern Instruments Nano ZS)] to find out the particles size distribution.

3.5 XRD of Calcined powder:

Calcined powders of all composition were subjected to phase analysis by X-ray diffraction (REGAKU,JAPAN). This is done to know the different phases present in the calcined powder. The angle range was 15^0-80^0.and the scan mode 3^0/min using Cu Kα (0.154nm) radiation. Throughout the process, the generator voltage and current was fixed at 35KV and 25mA. Phases present in the samples was identified by the search-match facility available with Philips X`Pert High Score Software.

3.6 Pelletisation:

The Calcined powder was mixed with 3% PVA solution (for binding). It was mixed in an agate mortar and left to dry. After drying it was scraped and grounded to fine powder. The different compositions powder were separately packed after being weighed (around 0.7 gm).The powder was then pressed into pellets by uniaxial compaction with load of 4 ton and 90 seconds dwelling time.

3.6 Sintering of pellets:

Then pellets were sintered at different temperature (1350^0C.and 1400^0C) for a soaking period of 4 hours and taken for further characterization.1350^0C firing was done in a chamber furnace and 1400^0C firing was done in a raising hearth furnace. Platinum substrate was used for sintering. After firing pellets appearance were monitored.

.

3.7 Measurement of density:

The bulk densities of the sintered pellets were measured by Archimedes principle using vacuum method in Kerosene medium (specific, gravity. 0.81715). The dry weight, soaked weight and suspended weight were measured. The densities of pallets were calculated by formula:

Bulk Density = {dry weight/ (soaked weight – suspended weight)} *0.81

3.8 Micro structural analysis by FESEM:

The sintered pellets were taken for SEM analysis. FESEM (Field Emission Scanning Electron Microscope, Nova Nano SEM/FEI).instrument was used. The pellets were gold coated in a sputtering coater. Then they were loaded for analysis. This analysis helps us to know the complete microstructure of the sintered sample.

3.9 Dielectric Measurement:

For dielectric measurement, samples were polished by emery paper 400 microns and then ultrasonicated using acetone to wash away the fine debris on the pellet surface. The clean samples were electroded with silver paste followed by curing at 550^0C for 30min.Dielectric measurement was carried out using HIOKI LCR (3532-50) meter in frequency range of 42 Hz to 1MHz.

Dielectric behavior has also been studied as a function of temperature with the temperature ranging from room temperature to 100^oC. The samples were placed in between two platinum sheets each of which is connected to a platinum wire. The whole arrangement was covered with an alumina tube. A small force was applied by a spring to ensure good contact to the sample electrodes. The temperature of the specimen was controlled using a carbolite furnace at a heating rate of 2^oC/min.

The relative permittivity (ε_r) is calculated from the measured values of capacitance and physical dimension of the specimen. The relations are expressed as [Hewlett Packard, 1987]:

$$C = \frac{\varepsilon_0 \varepsilon_r A}{t}$$

where ε_r the relative permittivity of the piezoelectric material, ε_0 is the relative permittivity of free space (8.854×10^{-12} F/m), t is the distance between electrodes (m), A is the area of the electrodes (m^2).

3.10 Ferroelectric Measurement:

The Polarization hysteresis measurement (P-E loop) was carried out by an automatic P-E loop tracer (Marine India, Electronics). All the measurements were carried out at room temperature The polarization hysteresis measurements based on standard Sawyer- Tower circuit In order to avoid dielectric breakdown in air, silicon oil with a high dielectric strength is used to cover the sample. An approximate value of the electric field strength in the sample is obtained with the input voltage and the sample thickness.

3.11 Piezoelectric coefficient (d_{33}) measurement:

For the piezoelectric measurements, the pellet samples were first poled in silicon oil under an applied different field at room temperature for 20min. The pellets were poled in a silicon oil bath under a dc field of 800V/mm for 20min.The d_{33} coefficients of the poled samples were measured after 24h with a d_{33} meter (YE2730A d_{33} Meter, APC International Ltd.). A force of 0.25N is applied to the sample and the corresponding d_{33} coefficient is measured.

Process Chart

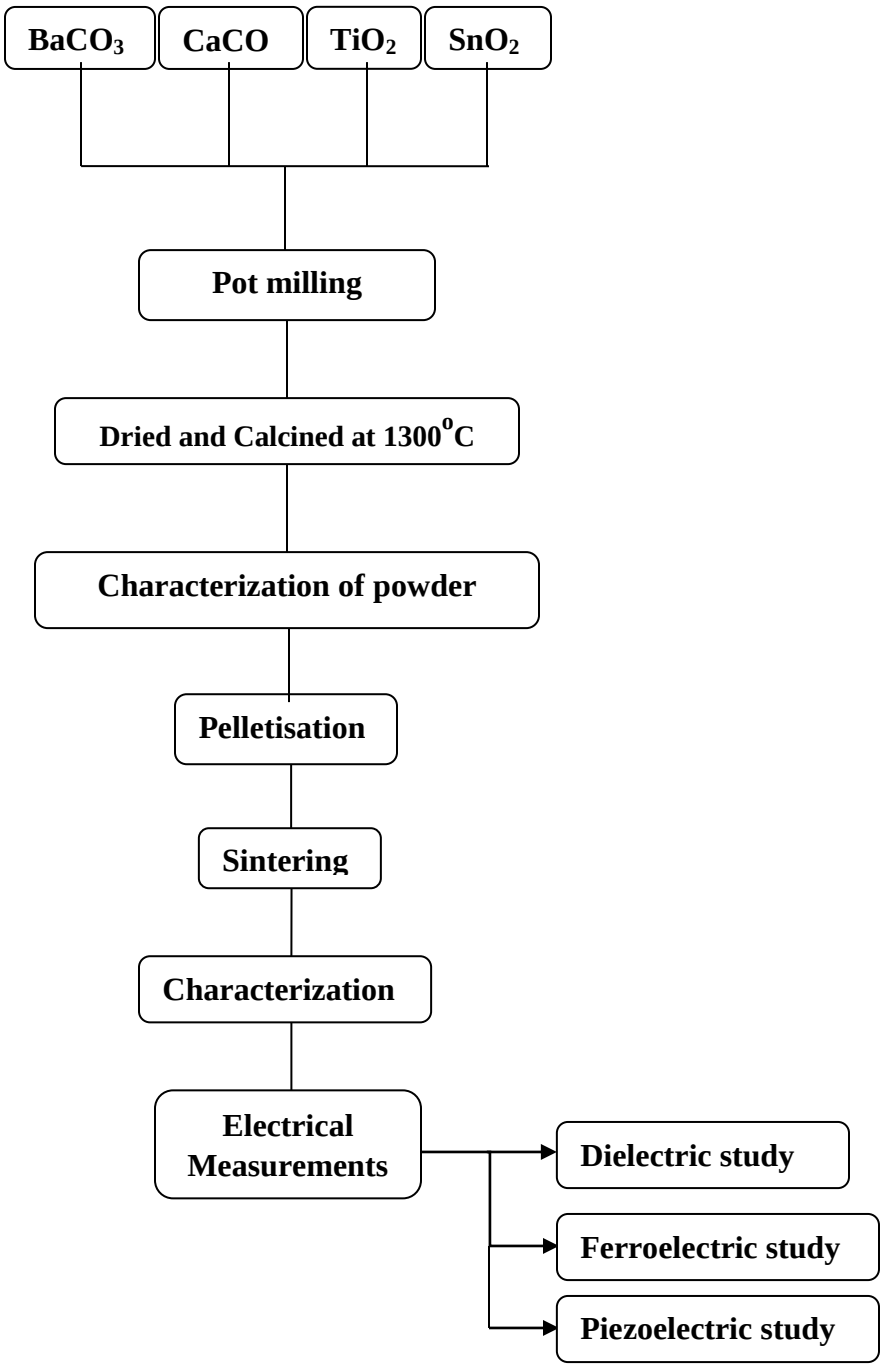

Figure 3.1 Process chart for synthesis & characterization

CHAPTER-4

RESULTS AND DISCUSSION

Results and discussion

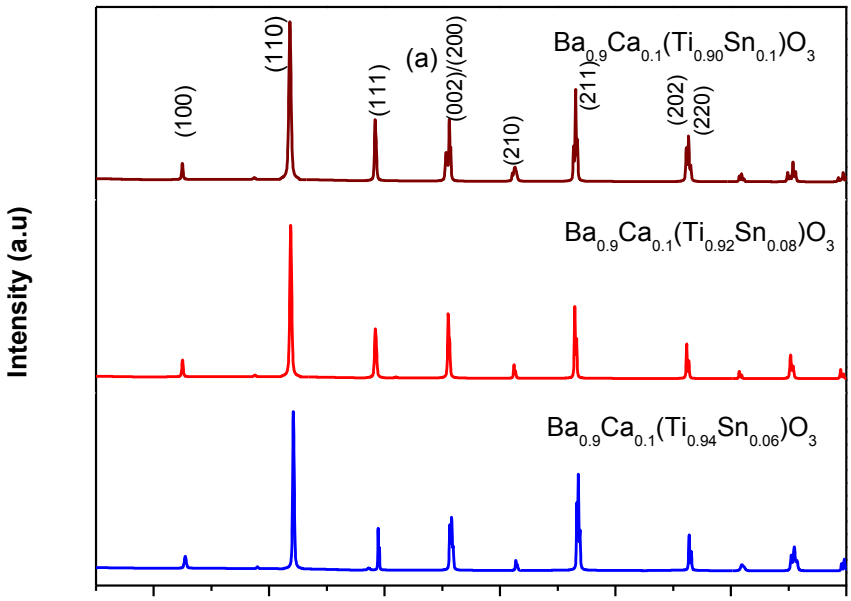

Figure 4(a): XRD analysis of powder samples calcined at 1300°C/4h

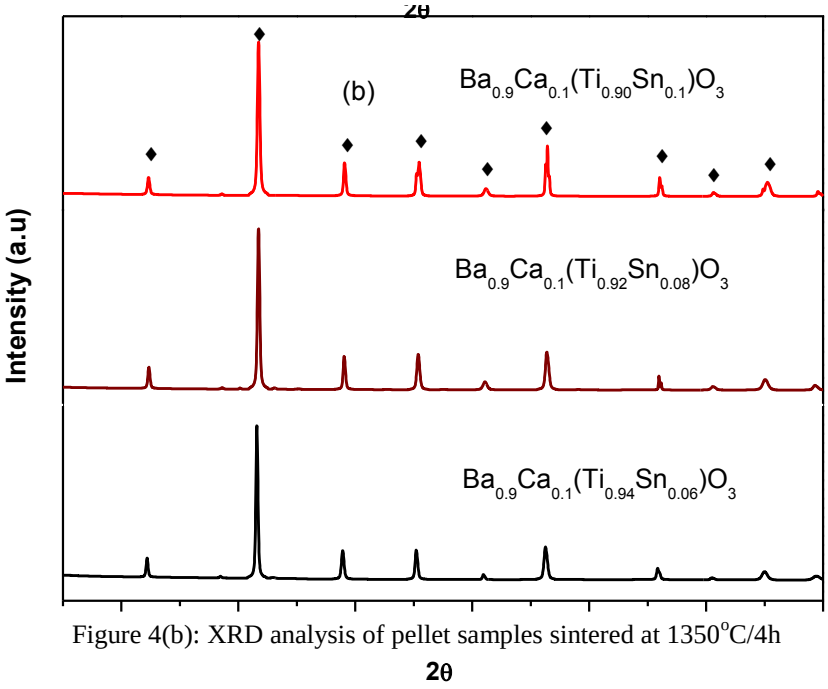

Figure 4(b): XRD analysis of pellet samples sintered at 1350°C/4h

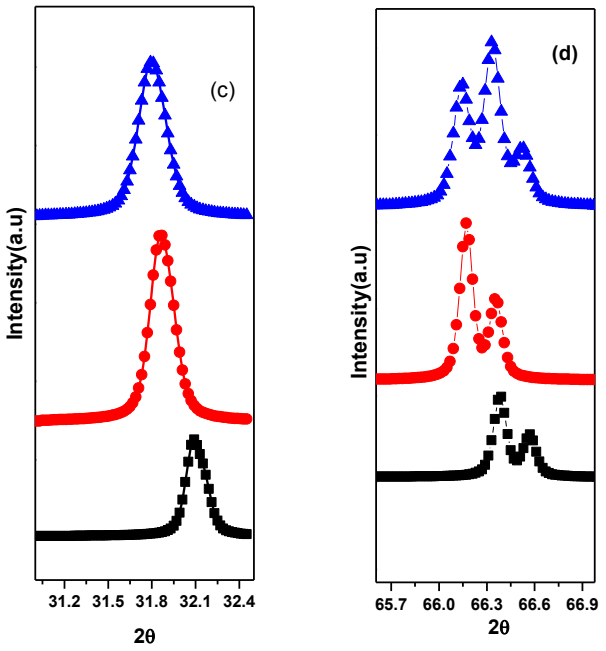

Figure 4(c) and (d): Selected region of X-ray diffraction patterns in the range of 31-32.5, 65-67^{o}.

Figure 4(a-d) X-ray diffraction patterns of $Ba_{0.9}Ca_{0.1}(Ti_{1-x}Sn_x)O_3$ceramic (a) calcined at 1300°C (b) sintered at 1350^{o}C/4hrs (c) and (d)selected region of X-ray diffraction patterns in the range of 31-32.5, 65-67^{o}.

Figure 4(a) shows the X-ray diffraction patterns of $Ba_{0.9}Ca_{0.1}(Ti_{1-x}Sn_x)O_3$ ceramics calcined at 1300^{o}C /4h. It can be observed that all compositions exhibit the pure perovskite structure and no secondary phase was observed. It suggests that Ca^{2+} and Sn^{4+} diffuse into the $BaTiO_3$ lattice to form a complete solid solution [25]. Figure 4(b) shows the X-ray diffraction patterns of $Ba_{0.9}Ca_{0.1}(Ti_{1-x}Sn_x)O_3$ceramics sintered at 1350^{o}C /4h. It is observed that all the compositions exhibit the perovskite structure. Moreover, it is clear from the magnified X-ray pattern in the range of 31-32.5^{o} that the position of the diffraction peaks shift towards the lower diffraction angles with increase in Sn^{4+} content. The shifting of the diffraction peaks to lower diffraction angles indicate the increase in lattice dimension and the distortion of crystal lattice. It may be due to the occupation of larger size Sn^{4+}(0.83 Å) in Ti^{4+}(0.605Å) site. X-ray analysis of $Ba_{0.9}Ca_{0.1}(Ti_{1-x}Sn_x)O_3$ shows presence of both tetragonal and orthorhombic phase, which is feature with splitting of the (002)/(200) peak at around 2θ of 44-46° and (220)/(202) peak around 2θ of 65-67°. It can also match with JCPDS No. 89-1428 and 81-2200 respectively

[22].The coexistence of tetragonal and orthorhombic phases at room temperature was also reported by the other researchers [24].

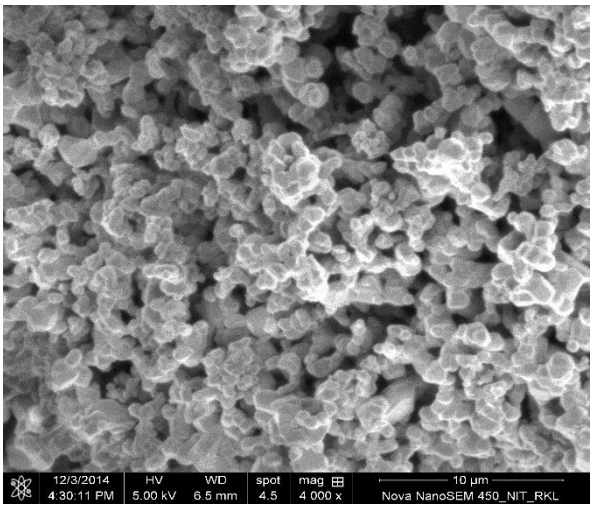

Figure 4.2: FESEM micrograph of the $Ba0.9Ca0.1(Ti0.94Sn0.06)O_3$ powder calcined at 1300°C/4h.

Figure 4.2 shows the FESEM micrograph of the $Ba_{0.9}Ca_{0.1}(Ti_{0.94}Sn_{0.06})O_3$ powder calcined at 1300°C. It can be observed that powders are agglomerated and spherical to irregular in shape with average particle size of 0.5-1µm.

Table-2(Bulk density of sintered pellets)

Composition	Bulk density (gm/cc)		Relative density (%)	
	1350/4h	1400/4h	1350/4h	1400/4h
$(Ba_{0.9}Ca_{0.1})(Ti_{0.94}Sn_{0.06})O_3$	5.47	5.34	91.1	89.0
$(Ba_{0.9}Ca_{0.1})(Ti_{0.92}Sn_{0.08})O_3$	5.58	5.54	93.0	92.3
$(Ba_{0.9}Ca_{0.1})(Ti_{0.90}Sn_{0.10})O_3$	5.34	5.11	89.0	85.2

Table-2 depicts the sintered density of the $Ba_{0.9}Ca_{0.1}(Ti_{1-x}Sn_x)O_3$ceramics at two different sintering temperatures of 1350°C and 1400°C. It was found that density increases with increase the Sn content up to x=0.08 after that decreases. The highest density was achieved in $Ba_{0.9}Ca_{0.1}(Ti_{0.92}Sn_{0.08})O_3$ceramic is 5.58gm/cc sintered at 1350°C which is more than 92 % of theoretical density. The density decreases with increase in sintering temperature from 1350°C to 1400°C.

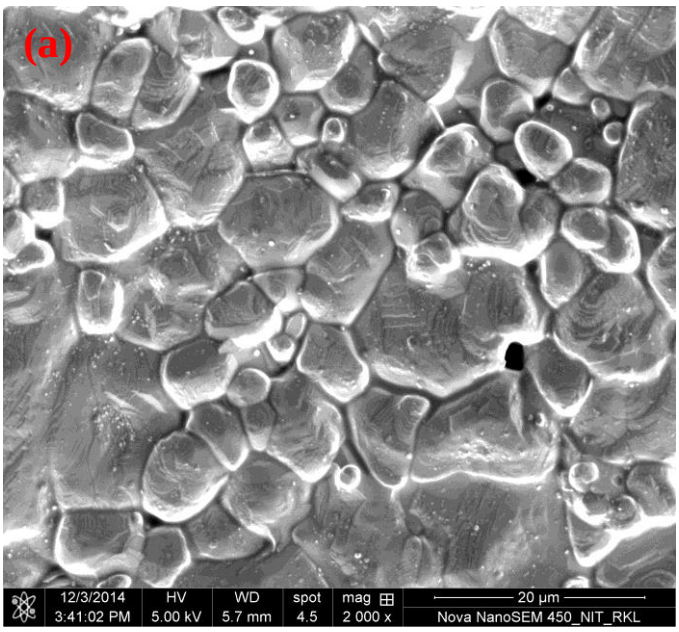

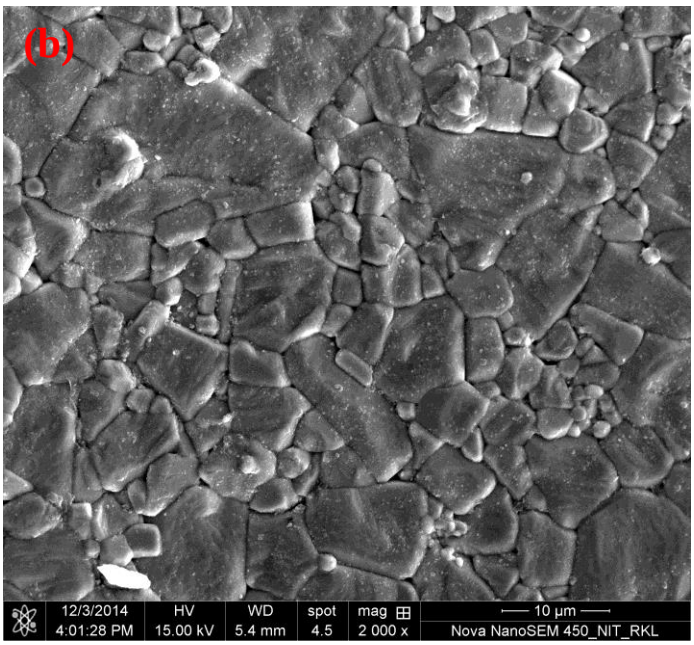

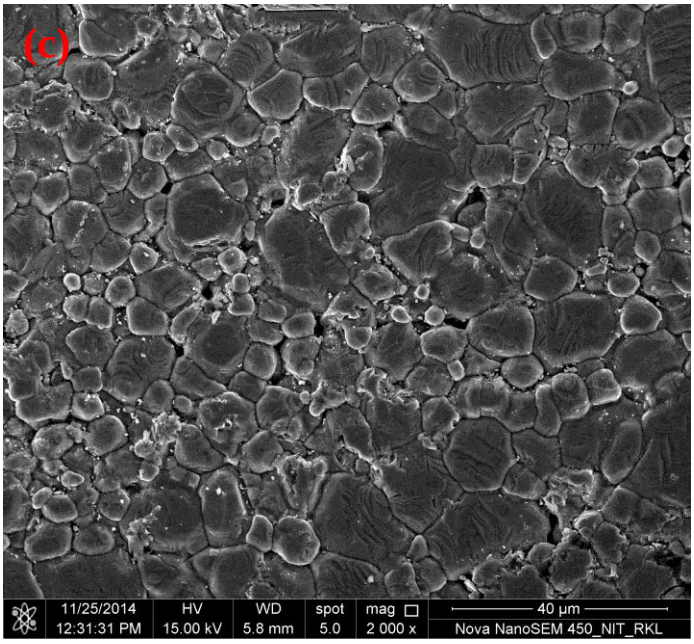

Figure 4.3 (a-c) FESEM micrographs of $Ba_{0.9}Ca_{0.1}(Ti_{1-x}Sn_x)O_3$ceramics sintered at 1350^{o}C/4h.

Figure 4.3 (a-c) shows the FESEM micrographs of $Ba_{0.9}Ca_{0.1}(Ti_{1-x}Sn_x)O_3$ ceramics sintered at 1350^{o}C for 4h.The average grain sizes are in the range of 5.5-11.8µm, 4.0-11.8µm, 5.9-15.6µm for x=0.06, x=0.08 and x=0.1, respectively. All the compositions show dense microstructures. The grain sizes are increases with increase in Sn content. The bimodal microstructure with big grain surrounded by many small grains are observed at x=0.06 which due to the discontinuous grain growth [26].

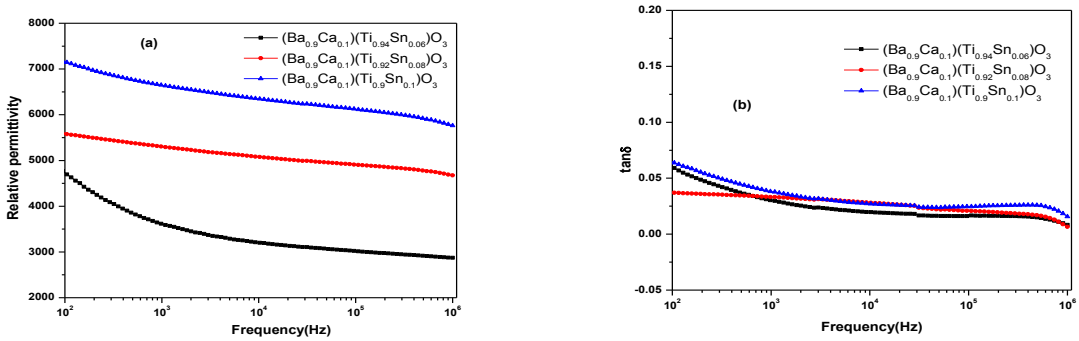

Figure 4.4 Room temperature relative permittivity and dissipation factor (tanδ) as the function of frequency for $Ba_{0.9}Ca_{0.1}(Ti_{1-x}Sn_x)O_3$ceramics sintered at 1350°C/4h

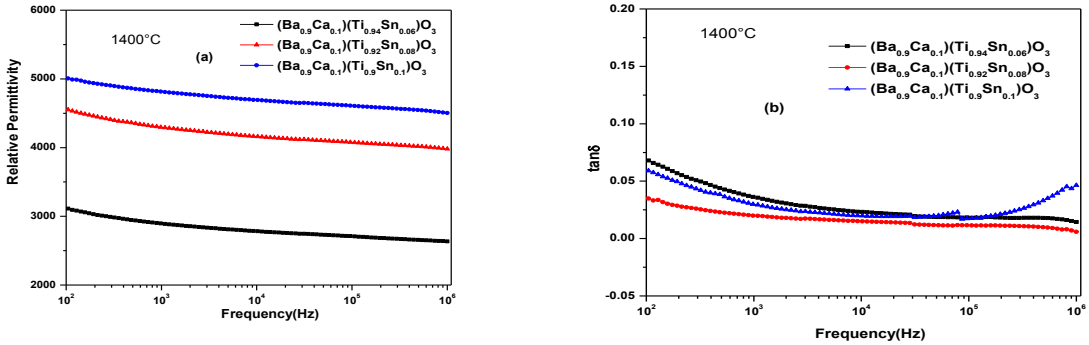

Figure 4.5 Room temperature relative permittivity and dissipation factor (tanδ) as the function of frequency for $Ba_{0.9}Ca_{0.1}(Ti_{1-x}Sn_x)O_3$ceramics sintered at 1400°C/4h.

Figure 4.4 shows the room temperature relative permittivity and dissipation factor (tanδ) as the function of frequency for $Ba_{0.9}Ca_{0.1}(Ti_{1-x}Sn_x)O_3$ ceramics sintered at 1350°C/4h. The Relative permittivity are 3588, 5293, 6632 for x=0.06, x=0.08 and x=0.1, respectively. It can be observed that the relative permittivity increases with increase in Sn content without the major change in loss tangent. These values are at par with that of reported result [27]. The relative permittivity and dissipation factor decreases with increasing sintering temperature as shown in fig 4.5. The lower relative permittivity at 1400°C may be due to lower density as compared to 1350°C sintered sample. The increment in permittivity with increase in Sn concentration can be explained by the increase in domain wall vibration (called the orientation polarization) and lattice vibration (ionic polarization) of the ceramics.

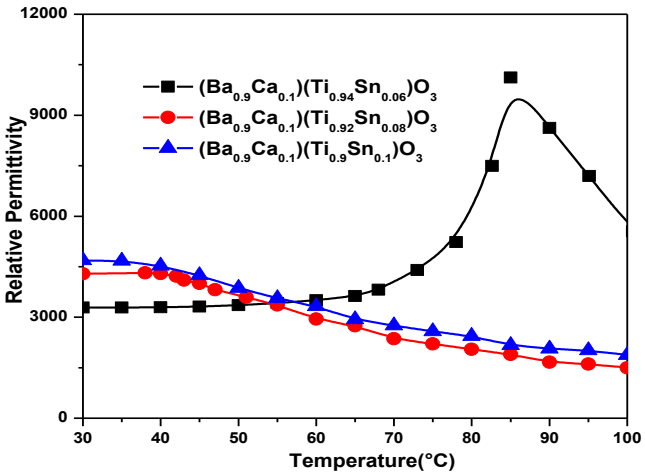

Fig 4.6 Temperature dependence of relative permittivity for the $Ba_{0.9}Ca_{0.1}(Ti_{1-x}Sn_x)O_3$ceramics.

Temperature dependence of relative permittivity for the $Ba_{0.9}Ca_{0.1}(Ti_{1-x}Sn_x)O_3$ ceramics is shown in Fig. 4.6.The phase transition (ferroelectric to paraelectric phase transition) temperature are 85°C, 40°C, 30°C for x=0.06, x=0.08 and x=0.1, respectively. With increasing content of Sn, the Curie point (T_c) shifts to lower temperature. These results are in good agreement with the

reported literatures [27]. Since Sn^{4+} has larger ionic size as compared to Ti^{4+}, the addition of Sn increases the chemical pressure imposed on the surrounding lattice and therefore results in lower T_c and lower maximum dielectric constant.

Table-3

Room temperature relative permittivity and dielectric loss of different compositions

Composition	Dielectric properties at room temp at 1kHz(1350°C)		Dielectric properties at room temp at 1kHz(1400°C)	
	εr	Tanδ	εr	tanδ
$(Ba_{0.9}Ca_{0.1})(Ti_{0.94}Sn_{0.06})O_3$	3588	0.029	2890	0.03
$(Ba_{0.9}Ca_{0.1})(Ti_{0.92}Sn_{0.08})O_3$	5293	0.033	4290	0.019
$(Ba_{0.9}Ca_{0.1})(Ti_{0.90}Sn_{0.10})O_3$	6632	0.037	4808	0.029

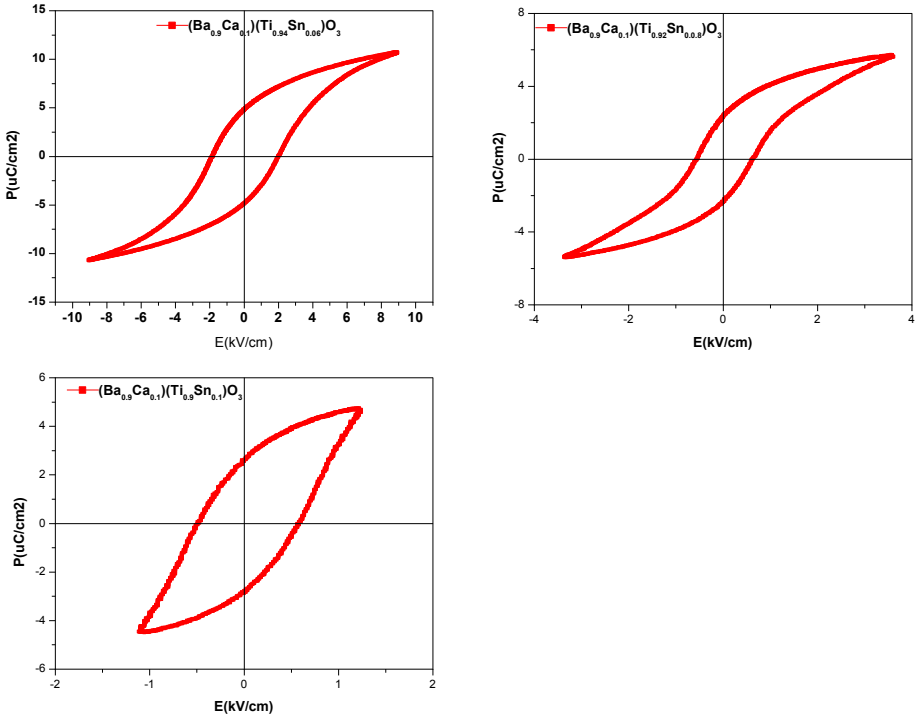

Fig 4.7 polarization-electric field characterization of the $Ba_{0.9}Ca_{0.1}(Ti_{1-x}Sn_x)O_3$ceramics at room temperature

Fig 4.7 shows the polarization-electric field characterization of the $Ba_{0.9}Ca_{0.1}(Ti_{1-x}Sn_x)O_3$ceramics at room temperature. It is found that the remnant polarization (P_r) and coercive fields (E_c) decreases with increasing Sn content. Well saturated hysteresis loops with regular shape can be observed for $Ba_{0.9}Ca_{0.1}(Ti_{0.94}Sn_{0.06})O_3$ceramics. Piezoelectric coefficient (d_{33}) value of $Ba_{0.9}Ca_{0.1}(Ti_{1-x}Sn_x)O_3$ceramics are shown in table 4. The d_{33} of $Ba_{0.9}Ca_{0.1}(Ti_{1-x}Sn_x)O_3$ceramics are 207,120 and 107pC/N for x=0.06, x=0.08 and x=0.1, respectively, which is lower than that of the reported literature [27]. The small grain size in the sintered sample may be the reason for lower d_{33} in our sample. The d_{33} value gradually decreases with increase in Sn content due to the appearance of more paraelectric phase in the sintered ceramics.

Table – 4

Ferroelectric and piezoelectric properties of sintered pellets

Composition fired at 1350°C/4h	**Ferroelectric properties at room temp at 50Hz**			**Piezoelectric Properties**
	Pr	**Ec**	**P_s**	**d_{33}**
$(Ba_{0.9}Ca_{0.1})(Ti_{0.94}Sn_{0.06})O_3$	4.9	1.87	10.72	207
$(Ba_{0.9}Ca_{0.1})(Ti_{0.92}Sn_{0.08})O_3$	2.32	0.49	5.72	120
$(Ba_{0.9}Ca_{0.1})(Ti_{0.90}Sn_{0.10})O_3$	2.52	0.46	4.80	109

CHAPTER-5

CONCLUSION AND REFERENCES

Conclusion:

$(Ba_{0.9}Ca_{0.1})(Ti_{1-x}Sn_x)O_3$ (x=0.06, 0.08 and 0.1) ceramics have been successfully prepared by a solid state method. Their phase formation, dielectric, ferroelectric and piezoelectric properties have been studied. It was found that the phase pure $(Ba_{0.9}Ca_{0.1})(Ti_{1-x}Sn_x)O_3$can be prepared at 1300°C by simple solid state mixing method. Powders can be sintered to more than 92% of the theoretical density at 1350^oC. The room temperature dielectric constant increases with increase in Sn^{4+} content and loss factor have less than 3.5%.The Curie temperature (T_c), piezoelectric coefficient, Pr and Ec decreases with increase in Sn^{4+} content. The highest piezoelectric coefficient (d_{33}=207pC/N) and dielectric constant (3588) was obtained for $(Ba_{0.9}Ca_{0.1})(Ti_{0.94}Sn_{0.06})O_3$ceramics. The results indicate that $(Ba_{0.9}Ca_{0.1})(Ti_{0.94}Sn_{0.06})O_3$ceramics are promising candidate for the lead-free piezoelectric applications.

References:

[1] A.J. Moulson, J.M. Herbert, Electroceramics—Materials, Properties, Applications Chapman & Hall, London, (1990).

[2] B. Jaffe, W. R. Cook Jr. and H. Jaffe, Piezoelectric Ceramics, Academic Press, New York (1971).

[3] Liu and Ren, Phys. Rev. Lett.**103**, 257602 (2009).

[4] Rodel J, Jo W, Seifert KTP, Anton EM, Granzow T,Damjanovic D, J. Am. Ceram. Soc. 92.1153–77 (2009) .

[5] Li J, Wang K, Zhu F, Cheng L, Yao F, J. Am. Ceram. Soc. 96 [12] 3677–3696 (2013)

[6] Y. G. Yao, C. Zhou, D. C. Lv, D. Wang, H. J. Wu, Y. D. Yang, and X.B. Ren, "Large Piezoelectricity and Dielectric Permittivity in $BaTiO_3$-x$BaSnO_3$ System: The Role of Phase Coexisting," EPL, 98, 27008, 6 pp (2012)

[7] J. Fousek, V. Janovec, J. Appl. Phys., **40**, 135–142, (1969). S. Stemmer, S. K. Streiffer, F Ernst, and M. R¨uhle, Philos. Mag. A, **71**, 713, (1995).

[8] D. Damjanovic, Rep. Prog. Phys., **61**, 1267–324, (1998).

[9] S. Singh, P. Singh, O. Parkash, D. Kumar, J. Alloys Compd., **493**, 522–528, (2010).;

[10]D.D. Gulwade, S. M. Bobade, A.R. Kulkarni, P. Gopalan, J. Appl. Phys., **97**, 074106, (2005).

[11] Dezhen Xue, Yumei Zhou, Huixin Bao, Jinghui Gao, Chao Zhou et al.; Appl. Phys. Lett. 99, 122901 (2011); doi: 10.1063/1.3640214

[12] Z.Q. Zhuang, M.P. Harmer, D.M. Smyth, R.E Newnham, Mater. Res. Bull., **22**, 1329,(1987).

[13]P.S.R. Krishna, D. Pandey, V.S. Tiwari, R. Chakravarthy, App. Phys. Lett., **62**, 231, (1992).

[14]V.S. Tiwari, N. Singh, D. Pandey, J. Am. Cream. Soc., **77**, 1813, (1994)

[15] R.C. Devries, R. Roy, J. Am. Ceram. Soc., **38**, 142, (1955

[16] D.A. Berlincourt, F. Kulesar, J. Acoust. Soc. Am., **24**, 709, (1952).

[17] T. Mitsul, W.B. Westphal, Phys. Rev., **124**, 1354, (1961)

[18] L. Zhang, O. P. Thakur, A. F. Gillian, M. K. Andrew, G. Mould, D. C. Sinclair, A R. West, Appl. Phys. Lett., **90**, 142914, (2007)

[19] G. A. Smolenskii, J. Phys. Soc. Jpn., **28**, 26, (1970). W. Chen, B. Liu, Q.F. Liu, S.T. Chen, J. Chin. Ceram. Soc., **28**, 1999, (2000)

[20] V.V. Shvartsman, W. Kleemann, J. Dec, Z.K. Xu, S.G. Lu., J. Appl. Phys., **99**, 124111, (2006)

[21] S.G. Lu, Z.K. Xu, H. Chen, Appl. Phys. Lett., **22**, 85–88, (2004). ,X. Wei, X. Yao, Mater. Sci. Eng. B., **137**, 184–8, (2007)

[22] Wei Li, ZhijunXu,† Ruiqing Chu, Peng Fu, and Guozhong Zang," Large Piezoelectric Coefficient in $(Ba_{1-x}Ca_x)(Ti_{0.96}Sn_{0.04})O_3$ Lead-Free Ceramics" J. Am. Ceram. Soc., 94 [12] 4131–4133 (2011).

[23] W. Li et al. / Journal of the European Ceramic Society 32 (2012) 517–520.

[24] Li-Feng Zhu, Bo-Ping Zhang, Xiao-Kun Zhao, Lei Zhao, Peng-FeiZhou, and Jing-Feng L," Enhanced Piezoelectric Properties of $(Ba_{1-x}Cax)(Ti_{0.92}Sn_{0.08})O_3$ Lead-Free Ceramics" J. Am. Ceram. Soc., 96 [1] 241–245 (2013).

[25] Markovic´ S, Mitric´ M, Cvjetic´anin N, Uskokovic´ D (2007) J Eur Ceram Soc 27:505.

[26] Frey M H, Payne D A. Grain size effect on structure and phase transformations for barium titanate. Phys Rev B 1996;54:3158–68.

[27] M. Chen et al. Polymorphic phase transition and enhanced piezoelectric properties in $(Ba_{0.9}Ca_{0.1})(Ti_{1-x}Sn_x)O3$ lead-free ceramics. Materials Letters 97 (2013) 86–89.